Observation of Precursor Magnetic Oscillations to the H-Mode Transition of ASDEX

K. Toi, J. Gernhardt, O. Klüber and M. Kornherr

IPP III/135 Mai 1988

MAX-PLANCK-INSTITUT FÜR PLASMAPHYSIK

8046 GARCHING BEI MÜNCHEN

Observation of Precursor Magnetic Oscillations to the H-Mode Transition of ASDEX

K. Toi, J. Gernhardt, O. Klüber and M. Kornherr

IPP III/135 Mai 1988

Observation of Precursor Magnetic Oscillations to the H-Mode Transition of ASDEX

K. Toi[(a)], J. Gernhardt, O. Klüber and M. Kornherr

Max-Planck-Institute für Plasmaphysik,

EURATOM-Association,

D-8046 Garching, München, Fed. Rep. Germany

Abstract

Precursor oscillations to the H-mode transition are identified in magnetic fluctuations of the ASDEX H-mode discharges initiated without a sawtooth. This precursor is m=4/n=1 mode, rotating with $f \simeq 10$ kHz in the opposite direction to co-injected neutral beams. Time behaviour of the amplitude suggests that the H-mode transition is caused, not by the edge electron temperature, but by the edge current density.

(a) Permanent address: Institute of Plasma Physics, Nagoya University, Nagoya 464, Japan

Since improved confinement regime, "H-mode", was discovered in a poloidal divertor tokamak ASDEX[1], several tokamaks[2-5] have achieved it in a divertor configuration. Recently, it has been observed also in limiter configuration[5]. On the H-mode discharge electron temperature and density near the plasma boundary (T_{eb}, n_{eb}) rise significantly *just after* the H-mode transition, but there is also a gradual rise in T_{eb} prior to the transition even in cases of the delayed transition. The H-mode transition is often initiated by a sudden rise in T_{eb} due to a sawtooth crash, which is interpreted by that T_{eb} reaches a certain threshold for the transition[6]. The initiation by a sawtooth mostly occurs at low heating power and high plasma current[7]. On discharges with high heating power in ASDEX, however, H-mode transition is often initiated without a sawtooth. H-mode discharges initiated without a sawtooth in PDX[8] exhibited that there was no simple threshold for H-mode transition in edge electron temperature. Alternatively to the requirement of a sufficiently high edge electron temperature, the H-mode could be triggered by the presence of a finite current density at the edge ($j_{\varphi b}$). We will try to analyze this aspect for the H-mode discharges of ASDEX (separatrix radius r_s=40 cm)[1], with the help of MHD modes detected by Mirnov probes. This work was inspired by the recent theoretical suggestion that the H-mode transition may be triggered by high $j_{\varphi b}$ in view of the stability of ideal ballooning modes[9], although the theory does not always succeed in explaining H-mode behaviors consistently.

In ASDEX, magnetic fluctuations ($\lesssim$100 kHz) are detected by Mirnov probes installed in a vacuum chamber. Ten probes cover the poloidal circumference by 44° at the inside and by 102° at the outside of the torus symmetric to the midplane[10,11]. Four probes are placed in the midplane outside the torus distributed over a toroidal angle of 156°. These signals ($\dot{B}_\theta$) are acquired by fast AD converter with 250 kHz sampling rate for 100 ms duration. H_α/D_α emission in a divertor chamber is also monitored by the fast AD converter to define the time of the H-mode transition more accurately.

Figure 1 shows temporal evolution of characteristic quantities of the H-mode discharge initiated without a sawtooth in a double null divertor configuration. In this discharge, H^0 beam power 3.45 MW is co-injected into a deuterium plasma of electron density $\overline{n}_e \simeq 3\times10^{13}$ cm^{-3} at a cylindrical safety factor $q_a \simeq 3.3$ (plasma current I_p=320 kA, toroidal field B_t=2.2 T, major radius $R\simeq167$ cm). The H-mode transition occurs at about 1.19 s, exhibiting the depression of H_α/D_α emission (I_α), rapid rise in soft X-ray emission at the plasma edge (I_{SXb}) and further rise in beta poloidal. Fluctuations of $\dot{B}_\theta$ and central soft X-ray emission (I_{SXo}) begin to rise about 35 ms before the transition. Only $\dot{B}_\theta$ inside the torus decreases obviously at the transition.

In order to investigate a fine structure of the fluctuations observed in $\dot{B}_\theta$ and I_{SXo}, frequency spectra are calculated for 1024 data points for about 4.1 ms. Figure 2 shows the frequency spectra of $\dot{B}_\theta$ inside the torus and I_{SXo} just before and after the H-mode transition. A peak at a frequency $f=f_o$ in a spectrum of I_{SXo} corresponds to m=1/n=1 internal mode, and the other peaks at $f=2f_o$ and $3f_o$ to the higher harmonics such as m=2/n=2 (Fig.2(a) and (c)). These modes are localized inside a q=1 surface. In a spectrum of $\dot{B}_\theta$, a characteristic peak is found at the same frequency ($f=f_o$, $2f_o$, and $3f_o$) as that of the internal mode (Fig.2(b) and (d)). Most interesting oscillation peak is that at $f=f_*$, which appears clearly only in the spectrum of $\dot{B}_\theta$ during L-phase (Fig.2(b)). Only the intensity of this peak is reduced in the H-phase in contrast to the other peaks.

We extract each characteristic frequency component from observed fluctuations by using an ideal filter method which is based on Fast Fourier Transform (FFT). The essential procedure of this method is as follows; (1) calculate a frequency spectrum by FFT, (2) separate the spectrum into three parts ($0 \leqq f \leqq f_L$, $f_L \leqq f \leqq f_H$, and $f_H \leqq f$) by lower and higher cut-off frequencies (f_L, f_H), (3) make the spectral power in the frequency range to be filtered to be zero, (4) retransform the filtered frequency spectrum into time series data. By analyzing test data composed of three frequency components, the relative deviations of amplitude and phase are estimated to be less than 1% for each filtered component. This method makes possible to identify mode numbers m and n of each frequency component successfully. For the discharge analyzed here (Fig.1) high frequency (HF-) component of $\dot{B}_\theta$ with $f \simeq f_o$ is identified as m=2/n=1 mode. The higher frequency component of $\dot{B}_\theta$ with $f \simeq 2f_o$ is m=3/n=2 mode. This m=2/n=1 (or m=3/n=2) mode is considered to be a mode driven by m=1/n=1 (or m=2/n=2) internal mode through a toroidal coupling. Note that the driven mode is localized near a q=1 surface in contrast to linearly unstable m=2/n=1 or m=3/n=2 tearing mode[12]. These modes m=2/n=1 and m=3/n=2 propagate in the same direction with co-injected neutral beams. On the other hand low frequency (LF-) component with $f \simeq f_*$ (Fig.2(b)) is m=4/n=1 mode, and propagates in an electron diamagnetic drift direction which is opposite to that of the neutral beams. The observed frequency ($f \simeq 10$ kHz) is comparable to an electron diamagnetic drift frequency estimated from an electron kinetic pressure profile measured at the plasma edge. This mode will be localized very close to the separatrix, since a resonant surface of q = 4 is located there.

In Fig.3, we enlarge the transition phase shown in Fig.1 together with the HF- and LF-components of $\dot{B}_\theta$ derived from the above mentioned ideal filter method. We obviously see the time sequence of events related to the H-mode transition. First, the amplitude of the m=4/n=1 LF-component of $\dot{B}_\theta$ begins to decrease, and then the rise in I_{SXb} follows. Finally, the H_α/D_α emission I_α is depressed suddenly. The time lag of the depression from the beginning of the decrease in the LF-component amplitude is about 1 ms. As seen from Fig.3, the amplitude of the m=2/n=1 HF-component decreases only gradually across the transition. During L-phase, the amplitude of the m=4/n=1 LF-component inside the torus is about 2 - 4 times larger than that outside it (Fig.4). Namely, the poloidal distribution exhibits a pronounced contrast to that of the m=2/n=1 HF-component. Maximum fluctuation level $\tilde{B}_\theta/B_\theta$ at the probe position is ~0.1 % for the m=2/n=1 mode and ~0.2 % for the m=4/n=1 mode just prior to the transition.

The LF-component suppressed just prior to the H-mode transition is again destabilized about 0.2 ms prior to the L-mode transition (from H- to L-phase), having the same mode structure (m=4/n=1) and rotation direction. Note that β_p is ~1 at the H-mode transition and ~1.6 at the L-mode transition. Therefore, the excitation of the LF-component seems not to be due to β_p effect or pressure effect. This component also appears ~0.1-0.2 ms prior to the sudden rise in H_α/D_α emission related to edge localized mode (ELM) and persists during ELM. The LF-component is excited ~0.5-0.6 ms after a crash of edge soft X-ray emission, which may be due to a pressure driven mode. Note that the behavior of the LF-component is not necessarily addressed to as precursor to ELM.

The following instabilities are considered to be responsible for the observed LF-component: microtearing mode driven by ∇T_e, ballooning mode driven by ∇p, and tearing or kink mode driven by ∇j_φ. The first mode may be excluded because for the analyzed discharge shown in Fig.1 ∇T_e at the plasma edge estimated from Thomson scattering data does not change essentially during the L-phase when the LF-component appears. If a ballooning mode is a dominant reason for excitation of the LF-component, many modes with a different helicity may be destabilized and the fluctuation may become incoherent in contrast to the observed coherent oscillations. Tearing or kink mode seems to be a most probable candidate for the LF-component. However, no theoretical stability analysis of the instability in a realistic divertor configuration is reported so far, although a simple analysis predicts to be stabilized by the high shear region[13]. As pointed out in ref.14, divertor plasmas have two basically different MHD-stable current density profile options : (1) usual L-mode profile and (2) H-mode "pedestal" profile. When j_φ profile in L-phase evolves to that in H-phase via various profiles, some modes with m=2,3,4 and others may be destabilized, depending on a current density or ∇j_φ at the plasma edge. The experimental observation seems to be consistent with this conjecture. Note that j_φ profile begins to evolve already in the latter half of the preceding L-phase (Figs. 1 and 3). The effect of non-inductive current drive due to ∇p and injected beams is conjectured to be one of the mechanisms which evolve j_φ profile during the preceding L-phase. Magnetic probe data cover both L- and H-phases for the limited numbers of shots in the range of q_a~2.6-3.3. We have detected the same type of LF-component in discharges at q_a~2.6 as well as q_a~3.3 as shown in Fig.1. However, the LF-mode is not always observed in H-mode discharges of ASDEX. That may be reason why the excitation of the mode during L- to H-phase depends on q_a and j_φ profile complicatedly. Moreover, the mode may be deformed by a plasma pressure effect or be hidden by various pressure driven modes.

We have reported m=4/n=1 coherent magnetic oscillations observed just prior to the H-mode transition in this letter. This oscillation is interpreted to be a tearing or kink mode driven by a finite current density at the plasma edge. The amplitude of the m=4/n=1 mode begins to decrease about 1 ms before the depression of D_α/H_α emission. In conclusion, these results suggest that edge current density in addition to edge electron temperature also has a potentiality to trigger the H-mode transition.

The authors acknowledge members of ASDEX and NI teams for fruitful discussions. One of them (K. T.) would like to thank Dr. K. Grassie, Dr. O. Gruber, Dr. F. Wagner and Dr. K. Lackner for stimulating discussions. He also is grateful to Dr. D. Eckhartt, and Dr. F. Leuterer for continuing encouragements and hospitalities.

References

1) F. Wagner et al., Phys. Rev. Lett. 49,1408 (1982).

2) S. Kaye et al., J. Nucl. Mater. 121, 115 (1984).

3) J. Luxon et al., in Proceedings of the Eleventh International Conference on Plasma Physics and Controlled Nuclear Fusion Research, Kyoto, Japan, 1986 (IAEA, Vienna, 1987), Vol. 1, p.159.

4) A. Tanga et al., ibid., p. 65.

5) K. Odajima et al., ibid. p.151.

6) F. Wagner et al., J. Nucl. Mater. 121, 103 (1984).

7) M. Keilhacker et al., Plasma Phys. and Controlled Fusion, 26, 49 (1984).

8) R. Fonck et al., in Proceedings of the Fourth Symposium on Heating of Toroidal Plasmas, Rome, 1984, p.37.

9) C.M. Bishop, Nucl. Fusion 26, 1063 (1986).

10) J. Gernhardt et aL., Max-Planck-Institute für Plasmaphysik Report III/59, 1980.

11) O. Klüber et al., in Proceedings of the Thirteenth European Conference on Controlled Fusion and Plasma Heating, Schliersee, 1986, p.136.

12) J.A. Holmes et aL., Phys. Fluids 25, 800 (1982).

13) T.S. Hahm and P. H. Diamond, Phys. Fluids 30, 133 (1987).

14) C.Z. Cheng et al., Plasma Phys. 29, 351 (1987).

Figure Captions

Fig.1 Temporal evolution of soft X-ray emissions at the plasma center I_{SXo} ($r/r_s \simeq 0$) and edge I_{SXb} ($r/r_s \simeq 0.95$), poloidal magnetic fluctuations $\dot{B}_\theta$ outside ($\theta=180°$) and inside ($\theta=-22°$) the torus, H_α/D_α emission in the divertor chamber (I_α), electron temperature derived from second electron cyclotron emission at the halfway to the edge ($R-R_o \simeq -24$ cm), and β_p obtained from a diamagnetic loop. $\dot{B}_\theta$ at $\theta=-22°$ is considerably affected by a rectifier noise ($f \simeq 1$ kHz).

Fig.2 Frequency spectra of I_{SXo} and $\dot{B}_\theta$ inside the torus. The spectra are calculated for 1024 data points just before (1.1850 - 1.1891 s) and after (1.1900 - 1.1941 s) the H-mode transition.

Fig.3 Time evolution of I_α, I_{SXb}, unfiltered $\dot{B}_\theta$ inside the torus, the m=2/n=1 HF-component ($f \gtrsim 16$ kHz), and the m=4/n=1 LF-component ($4 \lesssim f \lesssim 16$ kHz) of the $\dot{B}_\theta$ signal. The arrows indicate the time characterizes an occurrence of obvious change.

Fig.4 Distribution of time averaged amplitude of the LF- and HF-components in $\dot{B}_\theta$ signal along the poloidal angle during L-phase (1.1850 - 1.1891 s), here 180° means outside the torus and 0° inside the torus in the midplane.

Fig. 1

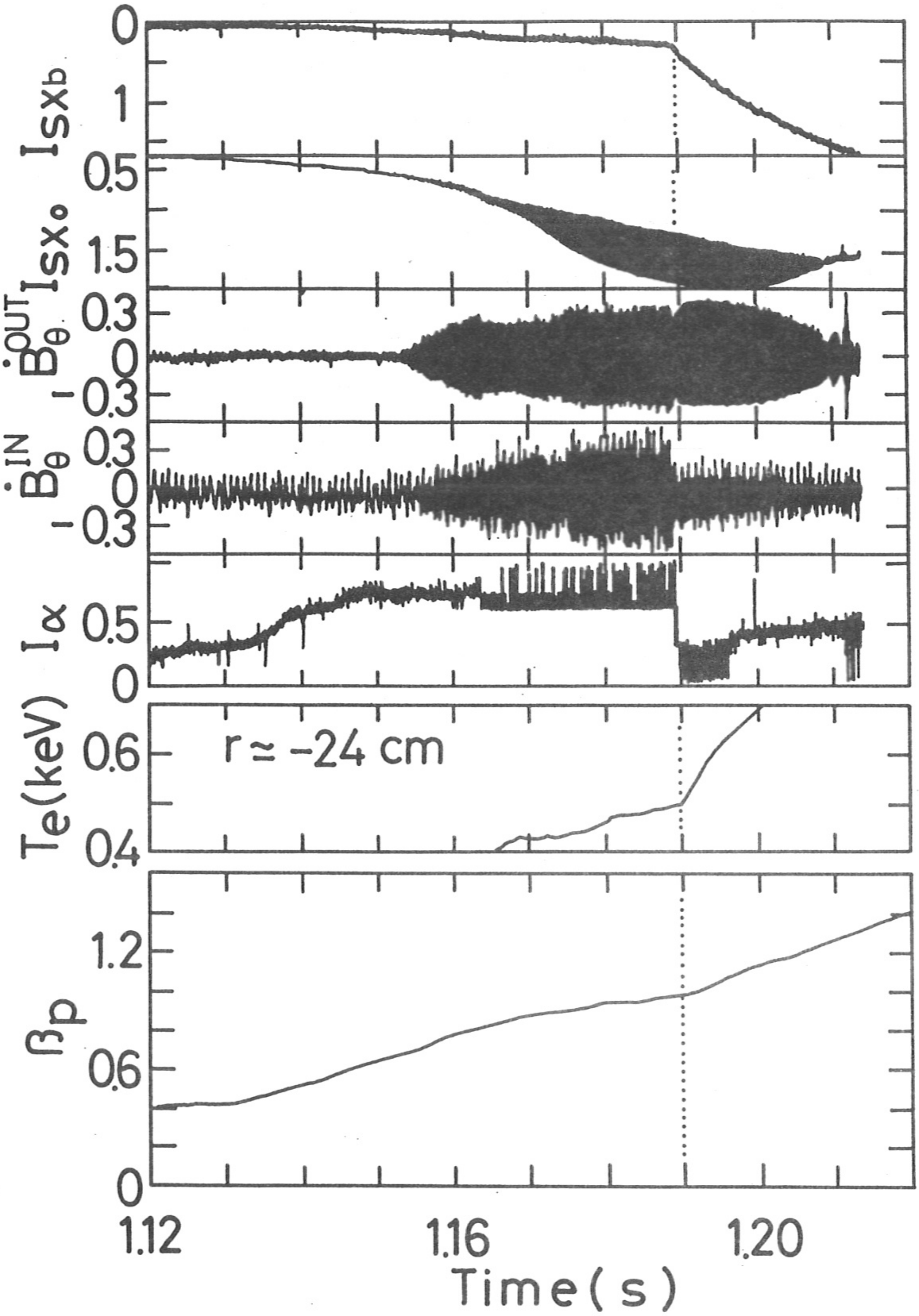

0
1
I_{SXb}
0.5
1.5
I_{SXo}
0.3
0
-0.3
$\dot{B}_\theta^{OUT}$
0.3
0
-0.3
$\dot{B}_\theta^{IN}$
I_α
0.5
0
T_e(keV)
0.6
0.4
r ≃ -24 cm
β_p
1.2
0.6
0
1.12
1.16
1.20
Time(s)

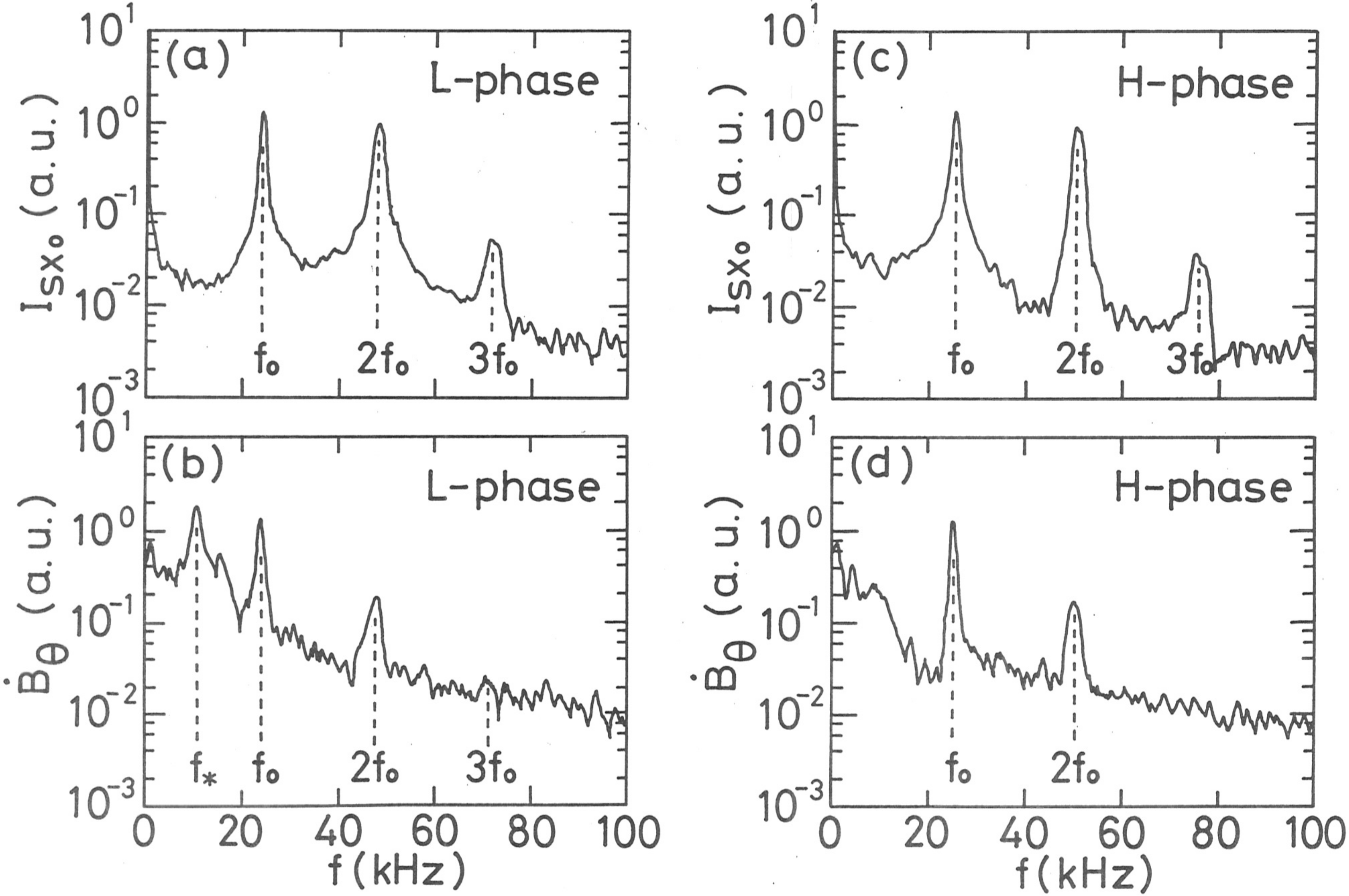

(a)
L-phase
(b)
L-phase
(c)
H-phase
(d)
H-phase
I_{SX_0} (a.u.)
$\dot{B}_\theta$ (a.u.)
10^1
10^0
10^{-1}
10^{-2}
10^{-3}
f_*
f_0
$2f_0$
$3f_0$
0
20
40
60
80
100
f (kHz)

Fig.2

Fig. 3

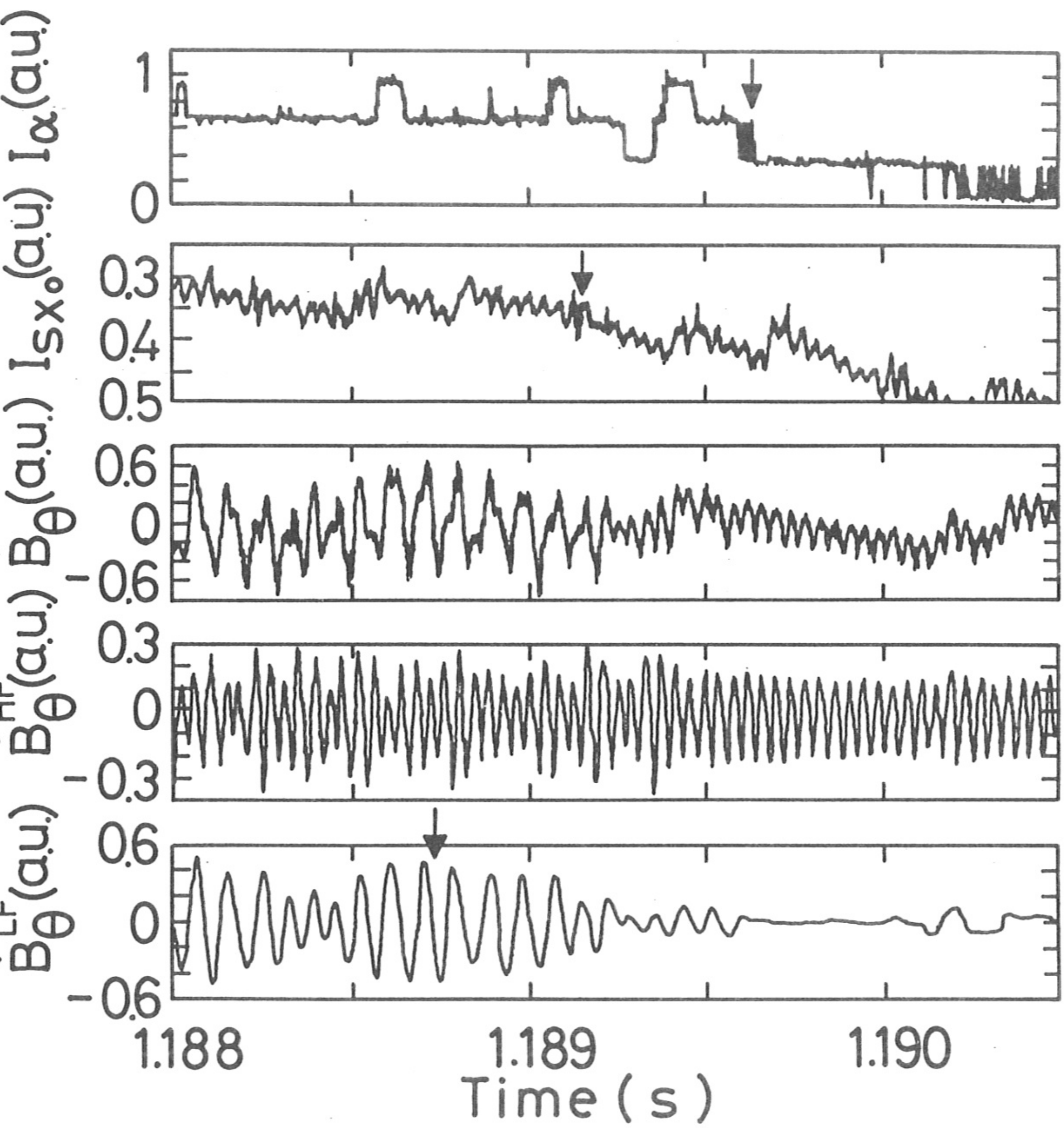

I_α(a.u.)
1
0
I_{SX_0}(a.u.)
0.3
0.4
0.5
$\dot{B}_\theta$(a.u.)
0.6
0
-0.6
$\dot{B}_\theta^{HF}$(a.u.)
0.3
0
-0.3
$\dot{B}_\theta^{LF}$(a.u.)
0.6
0
-0.6
1.188
1.189
1.190
Time (s)

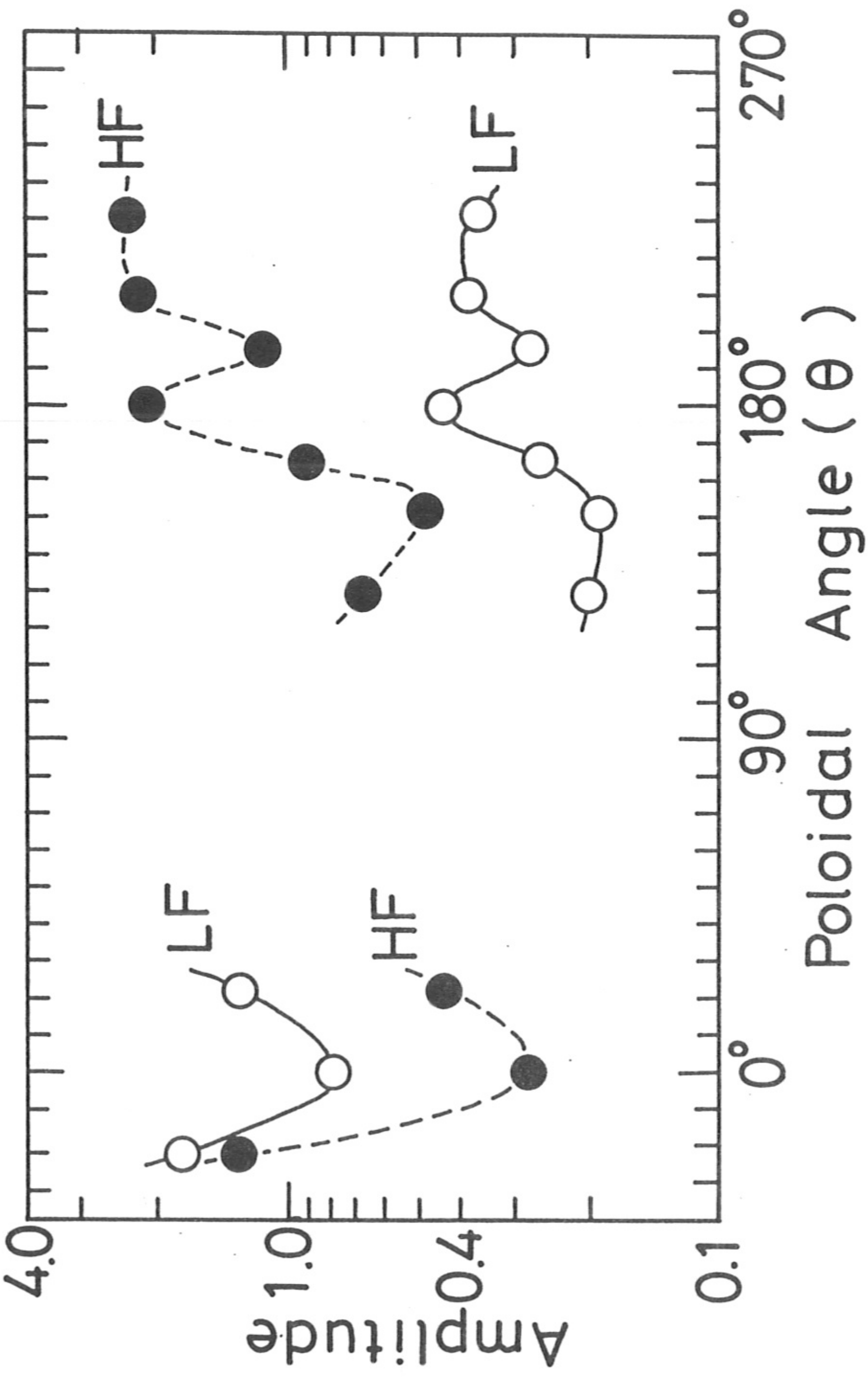

Fig.4